inter.noise 2014
MELBOURNE AUSTRALIA
16-19 NOVEMBER

The effect of flow on the natural frequencies of a flexible plate

Herwig Peters[1]; Li Chen[2]; Nicole Kessissoglou[1]

[1] School of Mechanical and Manufacturing Engineering, UNSW Australia, Sydney, NSW 2052, Australia.
[2] Maritime Division, Defence Science and Technology Organisation, Melbourne, Australia.

ABSTRACT

Vorticity induced vibrations (VIV) are caused by alternating vortices downstream of a structure, which result in a lift force acting on the structure perpendicular to the direction of the mean flow. This oscillating lift force excites vibrations of the flexible structure. When the vortex shedding frequency coincides with a natural frequency of the system, the structure vibrates at large transverse displacement amplitudes. These resonances occur at the natural frequencies of the overall system and are usually very different from the natural frequencies of the structure in vacuo or in a static fluid, which makes the prediction of the VIV resonances difficult. In this work, harmonic and transient simulations are used to predict the natural frequencies of a flexible plate in vacuo, in a static fluid, and in fluid flow. The results illustrate the effect of stationary and flowing water on the natural frequencies of a steel plate.

Keywords: Vorticity induced vibration, Hydrofoil I-INCE Classification of Subjects Number: 21.6.3

1. INTRODUCTION

When fluid flows past a hydrofoil, vortex shedding can occur behind the trailing edge. The vortex shedding leads to fluid forces acting on the surface of the hydrofoil which then vibrates and radiates noise. When the vortex shedding frequency coincides with the structural resonances of the hydrofoil in flow, vibration and sound radiation can reach large levels. Vorticity induced vibrations (VIV) have been studied extensively, in particular for the case of a cylinder in cross-flow (1, 2, 3). An important example of VIV of a cylinder in cross-flow are marine risers, which are a vertical pipeline from the sea floor to the production platform on the water's surface. Chaplin et al. (4) experimentally studied the vorticity induced response of a vertical tension riser subject to a stepped current. Vandiver et al. (5) measured the motion trajectories of waves travelling on long cylinders and showed that traveling wave VIV is dominant at high mode numbers. Zhao et al. (6) numerically investigated the vibration response of a two-dimensional, two degree of freedom cylinder close to a rigid wall.

Due to the importance of cylinders in cross-flow in engineering structures, many ways to control VIV have been researched. Roussopoulos (7) tried to control the vortices behind a rigid cylinder in air by means of two loudspeakers mounted below and above the cylinder in a wind tunnel. A similar experiment was repeated in a water channel, where the actuation to control the vortices was applied to the cylinder instead of the fluid. Park et al. (8) presented a computational study in which the control actuators are directly located on the cylinder, where they are used to modify the velocity field on the cylinder surface. Another idea was pursued by Ozono (9) who inserted a splitter plate behind the cylinder to interfere with the vortices in its wake region. For marine risers and other offshore applications, helical strakes that disturb the formation of vortices are often used to suppress VIV (10, 11).

A further important case of VIV is observed for flow along flat geometries, such as flat plates, airfoils and hydrofoils. Since the vortex shedding from a trailing edge is a mostly stable periodic process, the excitation of the structure occurs at an approximately constant frequency. Hence, the sound radiation from vibrating surfaces is also known as singing. The vortex shedding frequency is proportional to the flow speed over the structure. As the flow speed increases, so does the vortex shedding frequency. However, when the vortex shedding frequency excites a resonance the linear relationship between flow speed and vortex shedding frequency can break down and the vortex shedding frequency remains constant as the flow speed increases. This is known as lock-on. Blake (12) discusses the excitation of plates and hydrofoils by trailing edge vortices, and provides an upper bound of the VIV amplitude. Ausoni et al. (13, 14) present numerical and experimental results for a

[1] herwig.peters@unsw.edu.au

NACA0009 hydrofoil and the lock-on of the torsional mode of the flexibly mounted hydrofoil and the vortices. Ducoin et al. (15) experimentally studied a flexible hydrofoil with non-cavitating and cavitating flow. They found that the pulsating bubbles of the cavitating flow easily excite structural vibration and leads to increased displacement amplitudes of the hydrofoil.

The most common approach to reduce the level of vibration and radiated noise from airfoils and hydrofoils is the modification of the trailing edge geometry. Trailing edge treatments are used to break up the coherent vortex shedding, stopping the vortex shedding from reinforcing the structural vibration. Heskestad and Olberts (16) experimentally investigated flat blades with a range of symmetric trailing edge geometries and identified the rounded-tapered design and the notched design to exhibit the least vibration. Zobeiri et al. (17) experimentally compared the VIV of two NACA0009 hydrofoils with blunt and oblique trailing edges and showed how the coincidence of the lower and upper vortices leads to reduced vibration of the hydrofoil. This approach has been engineering practice for several years, as shown by HydroComp (18) and Fischer (19). New approaches to reduce VIV include serrated, poroelastic, adaptive and highly elastic trailing edges (20, 21, 22). These approaches have been primarily directed at the reduction of noise from airfoils due to turbulent eddies, but their application to hydrofoils also appears to be promising.

In this paper, computational fluid dynamics (CFD) and the finite element method (FEM) are used to study vorticity induced vibrations (VIV). The hydrofoil is approximated by a flexible plate with a blunt trailing edge and clamped at the leading edge. The effect of stationary and non-stationary fluid on the natural frequencies of the hydrofoil is examined.

2. NUMERICAL MODEL

A 2D model of a flat plate with a round leading edge and a blunt trailing edge is considered. The leading edge is fixed in space, while the plate and the trailing edge are free to vibrate in the x and y directions. A schematic diagram for the plate is shown in Figure 1 and the material properties of the plate are given in Table 1.

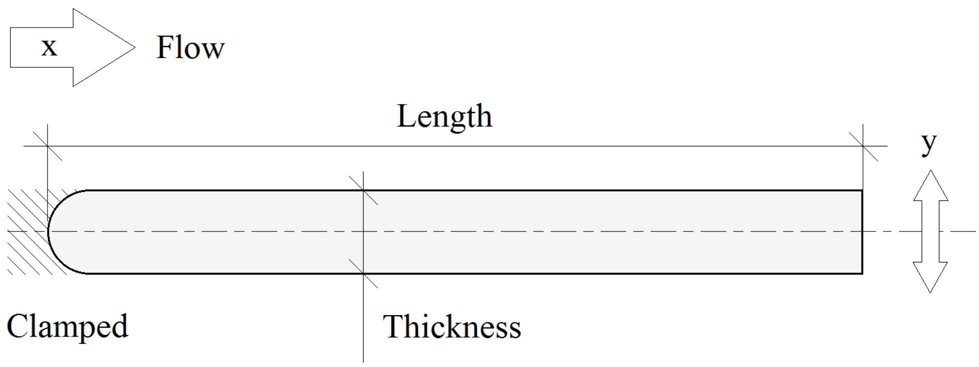

Figure 1 – Schematic diagram of the flexible plate

Table 1 – Dimensions and material properties of the plate

Parameter	Notation	Value	Unit
Length of plate	L	0.41	m
Thickness of plate	D	0.02	m
Aspect ratio of plate	L/D	20.5	-
Density of solid	ρ_s	7850	$^{kg}/_{m^3}$
Young's modulus of solid	E	variable	Pa
Poisson's ratio of solid	ν	0.3	-

The structural response of the fluid-loaded flat plate is obtained for the following three cases of the surrounding fluid:

1. Stationary air
2. Stationary water
3. Flowing water

2.1 Flat plate in stationary fluid

A 2D FEM model is created using the commercial software package COMSOL to obtain the structural response of the fluid-loaded flat plate excited by a point force. The point force with a magnitude of $F = 1\,\mathrm{N}$ is located at the trailing edge and orientated perpendicular to the mid-plane of the flat plate. The constant excitation frequency is chosen to be equal to the vortex shedding frequency obtained from the flat plate in flowing water, presented in the proceeding section. The unboundedness of the fluid surrounding the structure is approximated using a wave radiation boundary condition in the FE model (23). The material properties of the stationary fluids considered in this work corresponding to air and water are given in Table 2.

Table 2 – Material properties of the fluids

Parameter	Notation	Value	Unit
Density of air	ρ_{air}	1.205	$\mathrm{kg/m^3}$
Sound speed in air	c_{air}	343	$\mathrm{m/s}$
Density of water	ρ_{water}	1000	$\mathrm{kg/m^3}$
Sound speed in water	c_{water}	1500	$\mathrm{m/s}$

2.2 Flat plate in flowing water

A 2D fully coupled CFD/FEM model is developed using the commercial software package ANSYS 14.5. A transient CFD solver is coupled to a transient structural solver. The coupling between the fluid and the structure is achieved through the exchange of force and displacement data between the two solvers at each time step. For example, the CFD solver initially solves for pressure and fluid velocity in the fluid domain, and then passes the nodal forces acting on the fluid-structure interface to the structural solver. The structural solver uses the forces as an input to the structural model and solves for displacement, which in turn is passed back to the CFD solver to determine the updated position of the fluid-structure interface.

The CFD model parameters are listed in Table 3. The thickness-based Reynolds number is $\mathrm{Re}_D = 500$ and the length-based Reynolds number is $\mathrm{Re}_L = 10,250$. For the remainder of this study, the Reynolds and Strouhal numbers will be based on the characteristic length equal to the thickness of the flat plate as the vortex shedding is primarily determined by the body cross section (24). Since the flow across the flat plate is generally coherent in the spanwise direction for $\mathrm{Re}_D = 500$ (25), a 2D CFD model is sufficient to accurately predict the vortex shedding behind the trailing edge. The CFD and FEM meshes are shown in Figure 2. The shear stress transport (SST) k-ω turbulence model is used for the CFD model. The CFD mesh is structured close to the plate and for 0.6 m downstream from the trailing edge, and unstructured everywhere else. The first cell height has been chosen to achieve $y^+ \leq 1$ for the entire fluid-structure interface. A convergence analysis found a mesh with 37,860 CFD cells and a timestep of 0.1 s to be a reasonable spatial and temporal discretisation of the CFD domain. The structural domain is discretised with 1928 quadratic finite elements. The fully coupled transient analysis is run for 200 s, for which approximately 35 oscillations are observed.

Table 3 – CFD model parameters

Parameter	Notation	Value	Unit
Length of CFD domain	L_x	4.8	m
Height of CFD domain	L_y	1.61	m
Inlet velocity	v_{in}	0.025	$\mathrm{m/s}$
Outlet pressure	p	0	Pa
Dynamic viscosity of water	μ_{water}	0.001	$\mathrm{Ns/m^2}$

3. RESULTS

In this paper, the inlet velocity of the fluid in the CFD model is kept constant to achieve approximately constant flow conditions for a parametric study using a variable Young's modulus for the flat plate. Only the deformation of the vibrating plate affects the fluid flow. The Young's modulus of the plate is varied between 10^3 Pa and 10^7 Pa. Figure 3a compares the vibration amplitudes for the three cases introduced in Section 2. The vortext shedding frequency of the flat plate in flowing water as shown in Figure 3b is used as the excitation frequency for the plate submerged in a stationary fluid. The smallest, median and greatest value for the vortex

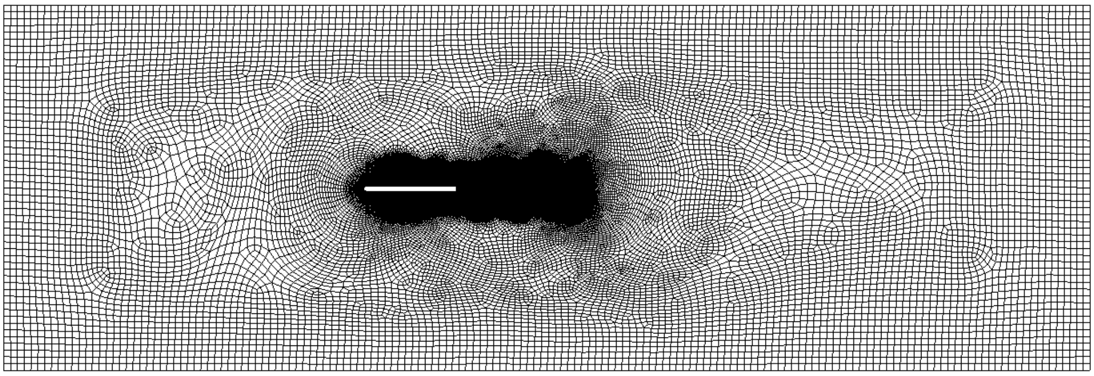

(a) CFD domain and overall mesh

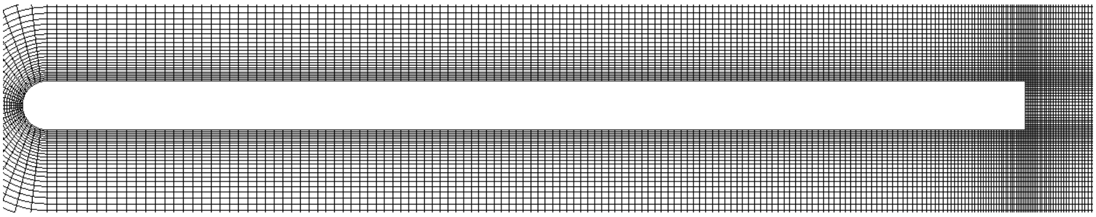

(b) CFD mesh close to the plate

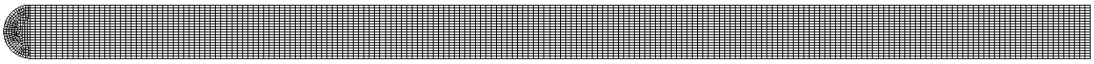

(c) FE mesh of the flexible plate

Figure 2 – Geometry and mesh of a flat flexible plate in flow

shedding frequency respectively is 0.18 Hz, 0.184 Hz and 0.192 Hz. Consequently, three lines are shown in Figure 3a to illustrate the variation of the vibration amplitude for the variation in the excitation frequency of the point force acting on the trailing edge of the plate.

Figure 3a shows the vibration amplitude of the trailing edge for the plate in stationary air, stationary water and flowing water. Each case exhibits three peaks that correspond to the first, second and third bending resonance of the plate for high, medium and low values of the Young's modulus, respectively. It is observed that the resonances occur at higher Young's moduli when the stationary fluid is changed from air to water, and remain unchanged when the fluid is changed from stationary water to flowing water. For the example presented here, it can be concluded that the increase of added mass due to dynamic fluid forces is negligible for low Reynold's number flow.

It is also observed that the width of the vibration amplitude peaks increases significantly for flowing water compared to the two stationary fluids. The increased width is predominantly due to the lock-on effect between the plate and the vorticies, which leads to the same resonant bending mode for a range of Young's moduli. The vibration amplitudes for the three cases are not directly comparable because the unit point force for the stationary fluid cases and the force due to the dynamic fluid pressure acting on the plate with flowing water are not equivalent.

The Strouhal number is given by $\mathrm{St} = fD/v_f$, where f is the vortex shedding frequency, D is the characteristic length and v_f is the velocity of the fluid. Vortex shedding frequencies of $f = 0.18$–0.192 Hz correspond to Strouhal numbers of $\mathrm{St} = 0.145$–0.155 as shown in Figure 3c. Considering the difference in geometry, this value agrees reasonably well to a Strouhal number of approximately $\mathrm{St} = 0.2$ for a cylinder in cross-flow in the published literature (26, 27), showing that the plate thickness is a reasonable choice for the characteristic length for the Strouhal number. Strouhal numbers of $\mathrm{St} = 0.145$–0.155 also agree reasonably well with the Strouhal number of $\mathrm{St} = 0.1865$ for a similar model with an aspect ratio of $L/D = 17.5$ and a Reynolds number of $\mathrm{Re}_D = 730$ published by Ryan et al. (24).

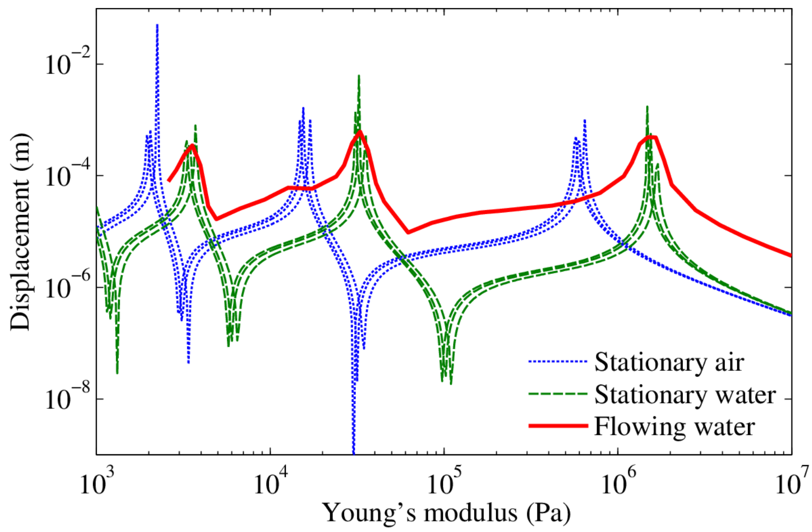

(a) Bending vibration amplitude of the trailing edge of the flat plate

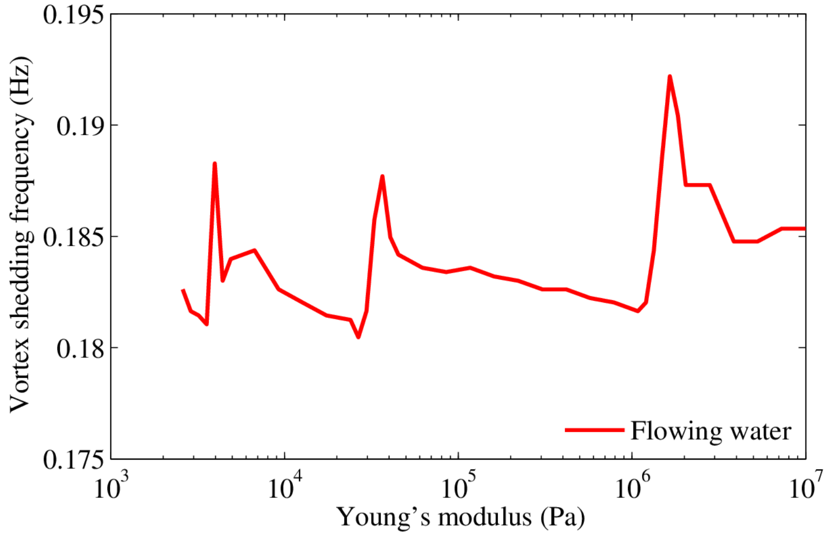

(b) Vortex shedding frequency for flow across the flat plate

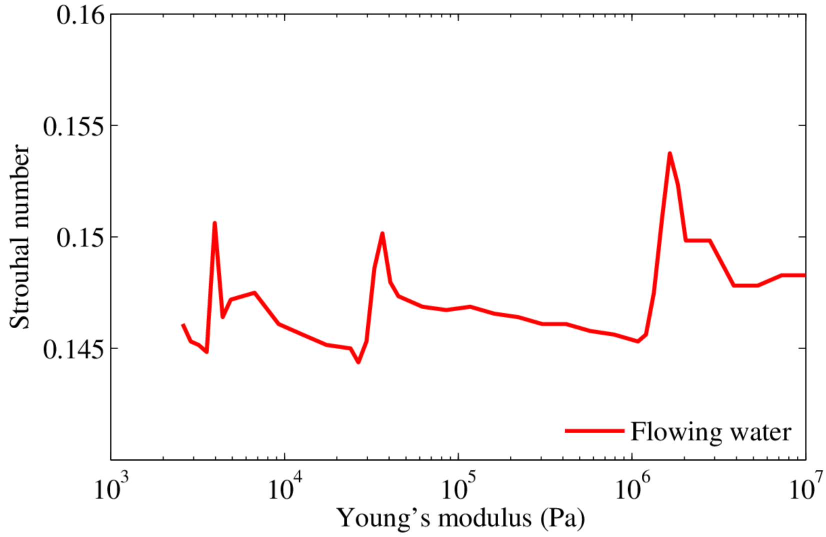

(c) Strouhal number for flow across the flat plate

Figure 3 – Results for the three cases of a plate in stationary air, stationary water and flowing water

4. CONCLUSIONS

The vorticity induced vibration of a flat plate in water as a function of the plate's Young's modulus has been presented. The VIV resonances have been compared to the resonances of the same plate fully submerged in two stationary fluids, water and air. It was observed that the resonant Young's modulus increases when the density of the stationary fluid increases from air to water. Considering a flowing fluid instead of a stationary fluid it was found that low Reynold's number flow does not significantly affect the resonant Young's moduli.

5. ACKNOWLEDGEMENTS

Compute time on the Leonardi High Performance Computing cluster at the Faculty of Engineering, UNSW Australia, is gratefully acknowledged. The first author gratefully acknowledges the financial assistance provided by the Australian Acoustical Society NSW Division to attend the Inter-Noise 2014 conference.

REFERENCES

1. Sarpkaya T. A critical review of the intrinsic nature of vortex-induced vibrations. J Fluids Struct. 2004;19:389–447.
2. Williamson CHK, Govardhan R. Vortex-induced vibrations. Annu Rev Fluid Mech. 2004;36:413–455.
3. Gabbai RD, Benaroya H. An overview of modeling and experiments of vortex-induced vibration of circular cylinders. J Sound Vib. 2005;282:575–616.
4. Chaplin JR, Bearman PW, Huarte FJH, Pattenden RJ. Laboratory measurements of vortex-induced vibrations of a vertical tension riser in a stepped current. J Fluids Struct. 2005;21:3–24.
5. Vandiver JK, Jaiswal V, Jhingran V. Insights on vortex-induced, traveling waves on long risers. J Fluids Struct. 2009;25:641–653.
6. Zhao M, Cheng L. Numerical simulation of two-degree-of-freedom vortex-induced vibration of a circular cylinder close to a plane boundary. J Fluids Struct. 2011;27:1097–1110.
7. Roussopoulos K. Feedback control of vortex shedding at low Reynolds numbers. J Fluid Mech. 1993;248:267–296.
8. Park DS, Ladd DM, Hendricks EW. Feedback control of von Kármán vortex shedding behind a circular cylinder at low Reynolds numbers. Phys Fluids. 1994;6:2390–2405.
9. Ozono S. Flow control of vortex shedding by a short splitter plate asymmetrically arranged downstream of a cylinder. Phys Fluids. 1999;11:2928–2934.
10. Zhou T, Razali SFM, Hao Z, Cheng L. On the study of vortex-induced vibration of a cylinder with helical strakes. J Fluids Struct. 2011;27:903–917.
11. Quen LK, Abu A, Kato N, Muhamad P, Sahekhaini A, Abdullah H. Investigation on the effectiveness of helical strakes in suppressing VIV of flexible riser. Appl Ocean Res. 2014;44:82–91.
12. Blake WK. Excitation of plates and hydrofoils by trailing edge flows. J Vib Acoust. 1984;106:351–363.
13. Ausoni P, Farhat M, Bouziad YA, Kueny JL, Avellan F. Kármán vortex shedding in the wake of a 2D hydrofoil: Measurement and numerical simulation. In: IAHR International Meeting of WG on Cavitation and Dynamic Problems in Hydraulic Machinery and Systems. Barcelona, Spain; 2006. .
14. Ausoni P, Farhat M, Escaler X, Egusquiza E, Avellan F. Cavitation influence on von Kármán vortex shedding and induced hydrofoil vibrations. J Fluids Eng. 2007;129:966–973.
15. Ducoin A, Astolfi JA, Sigrist JF. An experimental analysis of fluid structure interaction on a flexible hydrofoil in various flow regimes including cavitating flow. Eur J Mech B-Fluid. 2012;36:63–74.
16. Heskestad G, Olberts DR. Influence of trailing edge geometry on hydraulic-turbine-blade vibration resulting from vortex excitation. J Eng Gas Turb Power. 1960;82:103–109.
17. Zobeiri A, Ausoni P, Avellan F, Farhat M. How oblique trailing edge of a hydrofoil reduces the vortex-induced vibration. J Fluids Struct. 2012;32:78–89.

18. HydroComp. Singing propellers. A HydroComp Technical Report; 2005. Report 138.

19. Fischer R. The case of the singing propeller. Nav Archit. 2008;March 2008:70–71.

20. Moreau DJ, Doolan CJ. Noise-reduction mechanism of a flat-plate serrated trailing edge. AIAA Journal. 2013;51:2513–2522.

21. Jaworski JW, Peake N. Aerodynamic noise from a poroelastic edge with implications for the silent flight of owls. J Fluid Mech. 2013;723:456–479.

22. Madsen HA, Andersen PB, Andersen TL, Bak C, Buhl T. The potentials of the controllable rubber trailing edge flap (CRTEF). In: European Wind Energy Conference & Exhibition. Warsaw, Poland; 2010. .

23. Bayliss A, Gunzburger M, Turkel E. Boundary conditions for the numerical solution of elliptic equations in exterior regions. SIAM J Appl Math. 1982;42:430–451.

24. Ryan K, Thompson MC, Hourigan K. Three-dimensional transition in the wake of bluff elongated cylinders. J Fluid Mech. 2005;538:1–29.

25. Doddipatla LS. Wake dynamics and passive flow control of a blunt trailing edge profiled body. The University of Western Ontario; 2010.

26. So RMC, Savkar SD. Buffeting forces on rigid circular cylinders in cross flows. J Fluid Mech. 1981;105:397–425.

27. Schewe G. On the force fluctuations acting on a circular cylinder in crossflow from subcritical up to transcritical Reynolds numbers. J Fluid Mech. 1983;133:265–285.